

Laser frequency stabilisation via quasi-monolithic, unequal arm-length Mach-Zehnder interferometer with balanced DC readout

Oliver Gerberding^{1,*}, Katharina-Sophie Isleif^{2,†}, Moritz Mehmet^{1,2}, Karsten Danzmann^{1,2}, and Gerhard Heinzel¹

¹*Albert Einstein Institute, Max Planck Institute for Gravitational Physics,
Callinstrasse 38, 30167 Hannover, Germany and*

²*Institute for Gravitational Physics, Leibniz Universität Hannover, Callinstrasse 38, 30167 Hannover, Germany*

(Dated: November 1, 2016)

Low frequency high precision laser interferometry is subject to excess laser frequency noise coupling via arm-length differences which is commonly mitigated by locking the frequency to a stable reference system. This is crucial to achieve picometer level sensitivities in the 0.1 mHz to 1 Hz regime, where laser frequency noise is usually high and couples into the measurement phase via arm-length mismatches in the interferometers. Here we describe the results achieved by frequency stabilising an external cavity diode laser to a quasi-monolithic unequal arm-length Mach-Zehnder interferometer read out at mid-fringe via balanced detection. This stabilisation scheme has been found to be an elegant solution combining a minimal number of optical components, no additional laser modulations and relatively low frequency noise levels. The Mach-Zehnder interferometer has been designed and constructed to minimise the influence of thermal couplings and to reduce undesired stray light using the optical simulation tool IfoCAD. We achieve frequency noise levels corresponding to LISA-like (laser interferometer space antenna) displacement sensitivities below $1 \text{ pm}/\sqrt{\text{Hz}}$ and are able to demonstrate the LISA frequency pre-stabilisation requirement of $300 \text{ Hz}/\sqrt{\text{Hz}}$ down to frequencies of 100 mHz by beating the stabilised laser with an Iodine locked reference.

I. INTRODUCTION

Laser interferometry is the tool of choice for performing ultra-precise displacement and tilt measurements. One prominent subset of experiments is to apply such displacement measurements to free floating test masses to investigate effects of small forces and gravity itself. The most important recent achievements in this regard are certainly the direct detection of gravitational waves by the LIGO detectors [1] as well as the unprecedented low force noise levels demonstrated in the LISA Pathfinder satellite mission [2], a precursor for the space-based gravitational wave detector LISA [3]. The high displacement and angular sensitivities of laser interferometry have also motivated the implementation of the laser ranging instrument into the GRACE Follow-On mission to further improve the inter-satellite ranging for the determination of Earth's time-varying geoid [4]. Low frequency laser interferometry, as used in the above mentioned space missions, is often limited by laser frequency noise, which is typically increasing towards lower frequencies and couples into phase measurements via unequal arm-lengths.

Laser frequency stabilisation at low frequencies has been extensively researched for the above mentioned space missions [5], as well as for optical clocks [6] and other metrology experiments [7]. In comparison to such rather demanding stability requirements the laser frequency noise levels required for achieving $1 \text{ pm}/\sqrt{\text{Hz}}$ displacement sensing levels for local interferometers in satellites, prominently test mass readouts, are moderate, because they are driven by much shorter arm-length

differences. Due to the use of time-delay interferometry [8] these moderate levels are also sufficient as pre-stabilisation level for the LISA mission, which, even though it is expected to have the longest interferometer arm-lengths and arm-length differences of any laser interferometer so far, has been proposed to be operated with frequency stabilities in the order of $300 \text{ Hz}/\sqrt{\text{Hz}}$ (assuming an absolute arm-length ranging accuracy of about 1 m) at low frequencies [9]. The use of ultra-stable optical benches in a thermally stable environment on LISA Pathfinder, LISA and similar satellite missions has led to experiments using this displacement stability to implement laser stabilisations with intentional unequal arm-length interferometers as frequency sensors. Such techniques have been implemented and tested using kHz heterodyne interferometry [10, 11], they have been proposed and analysed for MHz heterodyne interferometry [9] and also optical cavities interrogated using a novel heterodyne readout technique have been used [12].

Here we have implemented a related type of laser frequency stabilisation scheme that uses an unequal arm-length Mach-Zehnder interferometer (MZI) with balanced homodyne DC readout constructed on a glass ceramic with a low thermal expansion coefficient. The main motivation to implement such a homodyne stabilisation is based on recent developments and renewed interest in interferometry techniques that rely on some form of self-homodyning [13–16], all of which are in some form compatible with this stabilisation scheme. Additionally, the balanced DC readout belongs to a class of straightforward techniques that do not require any type of modulations or AC readout electronics and thus it might be an interesting option also for other experiments requiring some form of frequency noise reduction.

* contact@olivergerberding.com

† katharina-sophie.isleif@aei.mpg.de

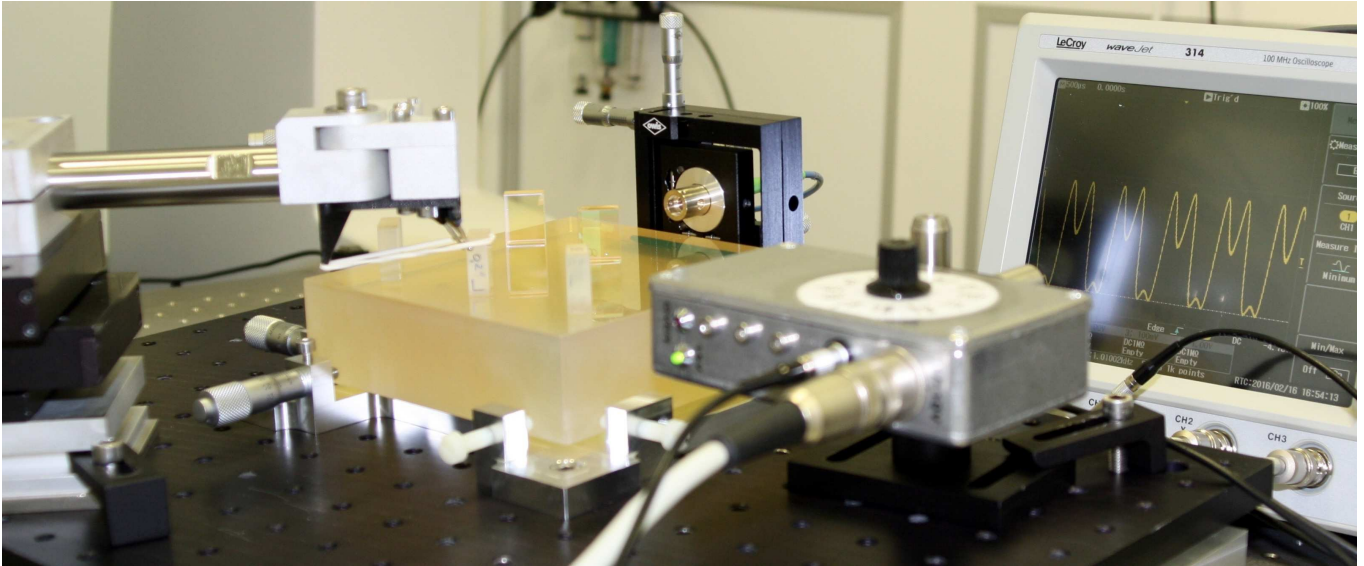


FIG. 1. Photograph of the construction of the Mach-Zehnder interferometer. Shown is the alignment stage of the recombination beam splitter using a pointing finger assembly while monitoring the interferometric contrast using a strong laser frequency modulation.

II. MACH-ZEHNDER DESIGN AND IMPLEMENTATION

The interferometer layout was designed using the C++ based optical simulation library IfoCAD aiming for an arm-length difference of about 12.5 cm. Numerical optimisations were used to minimise the influence of spurious beams generated by residual reflections at secondary surfaces. To this end the interferometer design includes two wedged beam splitters, enabling us to decouple secondary reflections by changing their propagation angles. A 2-dimensional interferometer layout generated by the software is shown in Figure 2. One additional feature of the interferometer is the third beam splitter placed behind the interference beam splitter to enable diagnostic so-called optical zero measurements.

The interferometer baseplate is made from Clearcam HS, a glass ceramic with a coefficient of thermal expansion of $0.1 \times 10^{-7} 1/K$ at ambient temperature, and with dimensions of 13.5 cm x 13.5 cm and a thickness of 3.6 cm. The light is brought onto the bench using a commercial fiber collimator, creating a collimated beam with a 1 mm waist radius, mounted in an adjustable tip-tilt, x-y mount. The mount itself is mounted on an adapter made from Invar that is glued using an epoxy to the side of the baseplate. The components are coated Fused Silica parts with a thickness of 7 mm.

The component alignment was done using a coordinate measurement machine and a combination of template-assisted positioning for uncritical components and an adjustable pointing finger assembly [17] for the recombination beam splitter. For the alignments of the input beam relative to the template we used an in-house developed beam measurement technique [18]. The bonding of the

components was done using an UV-cured optical adhesive that was applied using only minimal amounts of glue to achieve thin, planar bonding layers. Similar techniques have been implemented previously, for example based on a two-component epoxy [19]. The final recombination beam splitter alignment was done with a continuous contrast monitoring by applying a deep frequency modulation [14, 15], enabling straight forward optimisation with the adhesive already applied to the component before UV glueing. Figure 1 shows a photograph of this final assembly stage, achieving an optical contrast of more than 95% that remained constant during the UV cur-

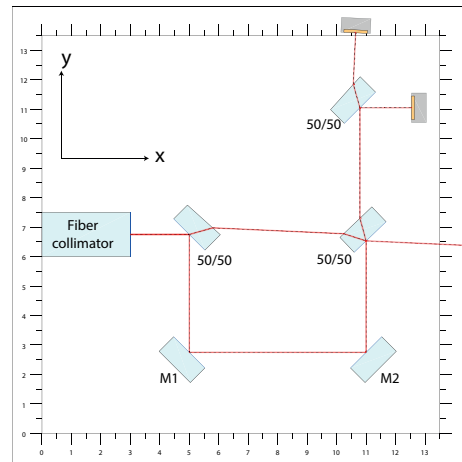


FIG. 2. Layout of the Mach-Zehnder interferometer with additional output splitting in the north output of the recombination beam splitter created using a 2D output of the IfoCAD c++ library.

ing, which took less than 2 minutes. No degradation of contrast was observed after four months of storage and operations, indicating also a decent long-term stability of the UV bond.

III. FREQUENCY STABILISATION SET-UP

To probe the displacement stability of the interferometer we placed it into a thermally isolated vacuum chamber and set up a balanced DC readout scheme, depicted in Figure 3. To achieve a balanced operation we employed a second, externally placed beam splitter in the east output and used its reflectivity dependence on the macroscopic beam incidence angle to achieve matched power levels on both photo diodes at the mid-fringe operation point. A low-noise, low-drift operational amplifier, in combination with ultra-stable photo diode bias voltages was implemented to perform a direct current subtraction followed by a high-gain trans-impedance amplification. The so generated sinusoidal output signal contains regular zero-crossings that can be used for locking without the need for subtracting an additional reference signal.

The so generated voltage was then used as input to a frequency stabilisation control loop that fed back to a rapidly tunable external cavity diode laser (ECDL, TLB-6821, New Focus, [20]) situated outside the vacuum chamber connected to the interferometer via a 14 m long fiber. Around 5% of the light was picked off and fed into a fiber beam splitter, interfering it with light from an iodine stabilised non-planar ring oscillator (NPRO) laser [21] that is used as frequency reference. Using a tunable demodulation scheme we measured the beat note frequency stability using a digital phase measurement system [22]. Given an arm-length difference of $\Delta l = 12,5$ cm of the MZI, which we confirmed using a measurement of the free spectral range of the interferometer, we can use the measured frequency fluctuations δf to determine the effective displacement noise δl using the laser wavelength $\lambda_0 \approx 1064.5$ nm and the speed of light c .

$$\delta l = \Delta l \times \frac{\delta f}{f_0} = \Delta l \times \frac{\delta f \lambda_0}{c} \quad (1)$$

By reversing this calculation we can also calculate the frequency noise level that is required to achieve a displacement noise of $1 \text{ pm}/\sqrt{\text{Hz}}$, the standard goal for the local interferometry in LISA and LISA Pathfinder. This level is $4.5 \text{ kHz}/\sqrt{\text{Hz}}$, taking into account an additional factor of two in the displacement sensing that is gained by using a reflection set-up. If it is proven that the Mach-Zehnder can provide this level of stability it will be a suitable frequency reference for interferometer set-ups that aim for the same level of displacement noise and use equivalent or shorter arm-length differences.

To probe the full performance level of this stabilisation scheme we immediately implemented a number of known techniques that have been crucial for achieving the performance in LISA breadboarding experiments [10]. This

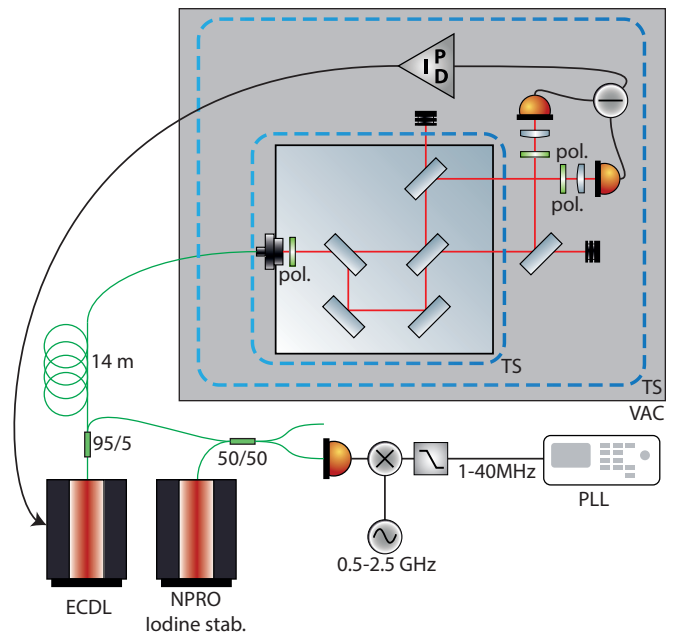


FIG. 3. Sketch of the frequency stabilisation experiment. The optical set-up outside the vacuum chamber (VAC) consisted of single-mode, polarisation maintaining fiber components. The beat frequency was first mixed down to 1 MHz to 40 MHz and then tracked by a digital phase-locked loop (PLL) implemented in a LISA-like phasemeter. The vacuum level during the experiment was on the order of 5×10^{-6} mbar. The interferometer and the analogue electronics were placed inside a thermal shield (TS), mounted in the vacuum chamber via thermally isolating feet. An additional thermal shield was placed around the baseplate of the interferometer and extended to cover the fiber coupler with multi-layer insulation foil. The heat generated by the electronics is understood to be the main driver of the observed long-term drifts, with a thermal equilibrium still not achieved after a week of pumping. The optical input power of the interferometer was on the order of 10 mW.

includes prominently the placement of thin-film polarizers with ultra-high extinction ratio after the fiber coupler and in front of both photo diodes to reduce the influence of parasitic interferences due to residual beams in the undesired, orthogonal polarisation. Additionally we made use of focussing lenses in front of the photo diodes to reduce beam-walk effects and we thermally isolated the long fibers routed outside the vacuum chamber using passive means. The experiment was placed inside a thermal shield, mounted via thermally resistive materials in a vacuum chamber with an additional passive thermal isolation layer on the outside. The interferometer itself was covered by a second thermal shield with an attached temperature sensor and the fiber collimator and its mount were additionally covered with multi-insulation foil. The achieved temperature stabilities have been measured and corresponding linear spectral densities, computed after subtracting a constant linear drift, are shown in Figure 4.

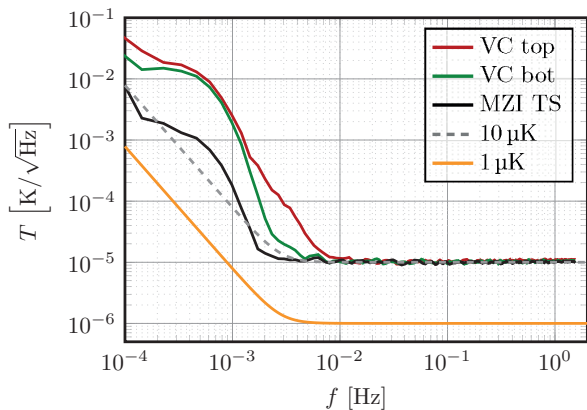


FIG. 4. Temperature spectral densities of the vacuum chamber and the MZI during the performance measurements. Shown are also the thermal stability goal for the LISA optical bench environment, a $1 \mu\text{K}/\sqrt{\text{Hz}}$ white noise relaxed towards lower frequencies, as well as a 10 times increased level for comparisons.

IV. RESULTS & DISCUSSION

The best frequency noise stability achieved with the current set-up is shown in Figure 5 in comparison to the free-running noise of the external cavity diode laser and the noise between two Iodine stabilised systems, that had been measured previously, indicating the fundamental performance limit of the set-up. At 1 Hz we reach this limit with $90 \text{ Hz}/\sqrt{\text{Hz}}$, which corresponds to a displacement noise of $40 \text{ fm}/\sqrt{\text{Hz}}$. The $4.5 \text{ kHz}/\sqrt{\text{Hz}}$ sensitivity (equivalent to $1 \text{ pm}/\sqrt{\text{Hz}}$) is achieved at all frequencies above 5 mHz, with a noise feature exceeding this level at lower frequencies. Some couplings due to vibrations and acoustics are visible at frequencies above 1 Hz and it is unknown whether this is introduced by the interferometer sensing or by excess fluctuations induced in the tunable diode laser that are not sufficiently suppressed by the loop gain. The unity gain frequency of the stabilisation was in the order of 1 kHz and mainly limited by the bandwidth of the frequency actuation piezo amplifier.

The excess noise observed at around 0.3 mHz was identified as outside excitation of our thermal environment, being clearly visible also in temperature sensors placed at the top and bottom of the inside of the vacuum chamber, as shown in Figure 4. Subtracting linear drifts from both the temperature measurement on top of our interferometer as well as the beat frequency measurement we find a correlated time-series shown in Figure 6 with a coupling factor of about $0.5 \text{ MHz}/1 \text{ mK}$. The predicted coupling based on the coefficient of thermal expansion of the base material and the arm-length difference is significantly below the observed value. Based on our IfoCAD simulations we assume that temperature fluctuations couple into the longitudinal phase measurement mainly via beam tilts. This is dominant in the interferometer due to

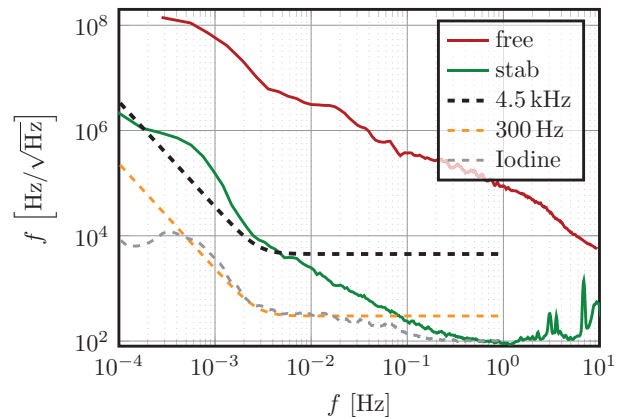


FIG. 5. Frequency spectral densities of the beat note between the Iodine stabilised NPRO laser and the ECDL, once free running and once stabilised to the MZI. Shown are also a frequency noise level of $4.5 \text{ kHz}/\sqrt{\text{Hz}}$ and the LISA frequency pre-stabilisation requirement of $300 \text{ Hz}/\sqrt{\text{Hz}}$. The graph also shows the frequency noise measured between two Iodine stabilised NPRO lasers, which is a measure for the lowest noise levels achievable with an Iodine stabilised reference [23]. The frequency readout noise floor (not shown) has been measured separately using only electronic signals and is on the order of $1 \text{ Hz}/\sqrt{\text{Hz}}$, slightly increasing towards lower frequencies.

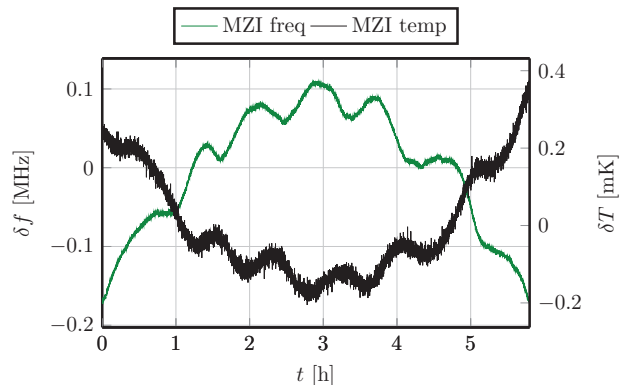


FIG. 6. Shown are the deviation of the measured beat frequency and the temperature measured at the thermal shield on top of the interferometer. A linear drift of 673.13 Hz/s and $0.96 \mu\text{K/s}$ respectively has been subtracted, as well as a mean value of the temperature of $25.66965 \text{ }^\circ\text{C}$.

the wedged components and the comparably high thermal coefficients of the commercial fiber collimator and its adjustable mount, as measured by Dehne et al. [10, 24] for such assemblies.

Even with this non-ideal input beam configuration we achieve the LISA frequency pre-stabilisation requirement down to 100 mHz. Extending this performance down to 1 mHz frequencies will require to include more stable, monolithic fiber collimators [25], or to further reduce the low frequency temperature fluctuations. A comparison of the measured levels with the thermal stabilities expected for LISA, as shown in Figure 4 is however quite encour-

aging that these levels could even be achieved with the current device.

A number of further improvements can be made to lower noise sources which are currently not identified to be limiting. These include the replacement of the Si photo diodes with devices based on InGaAs, largely increasing the photo diode responsivity and signal currents, hence reducing shot noise and electronic noise coupling. The addition of a local intensity stabilisation would also improve the robustness of the system against power fluctuations of the light provided to the interferometer. The current usage of additional beam splitters in the output ports does half the usable optical power but could also enable the implementation of redundant photo diodes, an alternative that might be considered for space applications.

ACKNOWLEDGMENTS

The authors would like to thank Daniel Penkert and Daniel Schütze for their help with the component positioning and beam measurement used for the interferometer construction. We would also like to thank Maike Lieser for supplying us with the reference measurement of the Iodine stabilised laser frequency noise. We also like to thank Stefan Ast for the help with the vacuum set-up.

The authors would like to thank the DFG Sonderforschungsbereich (SFB) 1128 Relativistic Geodesy and Gravimetry with Quantum Sensors (geo-Q) for financial support. We also acknowledge support by the Deutsches Zentrum für Luft- und Raumfahrt (DLR) with funding from the Bundesministerium für Wirtschaft und Technologie (Project Reference No. 50 OQ 0601)

Disclaimer: Certain commercial equipment, instruments, or materials are identified in this paper in order to specify the test and measurement procedure adequately. Such identification is not intended to imply recommendation or endorsement by the authors, nor is it intended to imply that the materials or equipment identified are necessarily the best available for the purpose.

-
- [1] B. P. Abbott *et al.* (LIGO Scientific Collaboration and Virgo Collaboration), *Phys. Rev. Lett.* **116**, 061102 (2016).
- [2] M. Armano, H. Audley, G. Auger, J. T. Baird, M. Bassan, P. Binetruy, M. Born, D. Bortoluzzi, N. Brandt, M. Caleno, L. Carbone, A. Cavalleri, A. Cesarini, G. Ciani, G. Congedo, A. M. Cruise, K. Danzmann, M. de Deus Silva, R. De Rosa, M. Diaz-Aguiló, L. Di Fiore, I. Diepholz, G. Dixon, R. Dolesi, N. Dunbar, L. Ferraioli, V. Ferroni, W. Fichter, E. D. Fitzsimons, R. Flatscher, M. Freschi, A. F. García Marín, C. García Marirrodriga, R. Gerndt, L. Gesa, F. Gibert, D. Giardini, R. Giusteri, F. Guzmán, A. Grado, C. Grimani, A. Grynagier, J. Grzymisch, I. Harrison, G. Heinzl, M. Hewitson, D. Hollington, D. Hoyland, M. Hueller, H. Inchauspé, O. Jennrich, P. Jetzer, U. Johann, B. Johlander, N. Karnesis, B. Kaune, N. Korsakova, C. J. Killow, J. A. Lobo, I. Lloro, L. Liu, J. P. López-Zaragoza, R. Maarschalkerweerd, D. Mance, V. Martín, L. Martin-Polo, J. Martino, F. Martin-Porqueras, S. Madden, I. Mateos, P. W. McNamara, J. Mendes, L. Mendes, A. Monsky, D. Nicolodi, M. Nofrarias, S. Paczkowski, M. Perreur-Lloyd, A. Petiteau, P. Pivato, E. Plagnol, P. Prat, U. Ragnit, B. Raïs, J. Ramos-Castro, J. Reiche, D. I. Robertson, H. Rozemeijer, F. Rivas, G. Russano, J. Sanjuán, P. Sarra, A. Schleicher, D. Shaul, J. Slutsky, C. F. Sopuerta, R. Stanga, F. Steier, T. Sumner, D. Texier, J. I. Thorpe, C. Trenkel, M. Tröbs, H. B. Tu, D. Vetrugno, S. Vitale, V. Wand, G. Wanner, H. Ward, C. Warren, P. J. Wass, D. Wealthy, W. J. Weber, L. Wissel, A. Wittchen, A. Zambotti, C. Zononi, T. Ziegler, and P. Zweifel, *Phys. Rev. Lett.* **116**, 231101 (2016).
- [3] K. Danzmann *et al.*, “The Gravitational Universe: Whitepaper for the” (2013).
- [4] B. S. Sheard, G. Heinzl, K. Danzmann, D. A. Shaddock, W. M. Klipstein, and W. M. Folkner, *Journal of Geodesy* **86**, 1083 (2012).
- [5] W. M. Folkner, G. de Vine, W. M. Kleipstein, K. McKenzie, R. E. Spero, R. Thompson, N. Yu, M. Stephens, J. Leitch, R. Pierce, T. T.-Y. Lam, and D. A. Shaddock, *ESTF*, *Earth Science* (2011).
- [6] T. Kessler, C. Hagemann, C. Grebing, T. Legero, U. Sterr, F. Riehle, M. Martin, L. Chen, and J. Ye, *Nature Photonics* **6**, 687 (2012).
- [7] T. Schuldt, K. Dringshoff, A. Milke, J. Sanjuan, M. Gohlke, E. V. Kovalchuk, N. Grlebeck, A. Peters, and C. Braxmaier, *Journal of Physics: Conference Series* **723**, 012047 (2016).
- [8] M. Tinto and S. V. Dhurandhar, *Living Reviews in Relativity* **8**, 1 (2005).
- [9] B. S. Sheard, G. Heinzl, and K. Danzmann, *Classical and Quantum Gravity* **27**, 084011 (2010).
- [10] M. Dehne, M. Tröbs, G. Heinzl, and K. Danzmann, *Opt. Express* **20**, 27273 (2012).
- [11] G. Heinzl, V. Wand, A. Garcia, O. Jennrich, C. Braxmaier, D. Robertson, K. Middleton, D. Hoyland, A. Rüdiger, R. Schilling, *et al.*, *Classical and Quantum Gravity* **21**, S581 (2004).
- [12] J. Eichholz, D. B. Tanner, and G. Mueller, *Phys. Rev. D* **92**, 022004 (2015).
- [13] A. Sutton, O. Gerberding, G. Heinzl, and D. Shaddock, *Opt. Express* **20**, 22195 (2012).
- [14] O. Gerberding, *Optics Express* **23**, 14753 (2015).
- [15] K.-S. Isleif, O. Gerberding, T. S. Schwarze, M. Mehmet, G. Heinzl, and F. G. Cervantes,

- Opt. Express **24**, 1676 (2016).
- [16] T. Kissinger, T. O. Charrett, and R. P. Tatam, Opt. Express **23**, 9415 (2015).
- [17] D. Penkert, *Hexagon - An Optical Three-Signal Testbed for the LISA Metrology Chain*, Diploma thesis, Leibniz Universität Hannover (2016).
- [18] D. Schütze, V. Müller, and G. Heinzel, Appl. Opt. **53**, 6503 (2014).
- [19] T. Schuldt, M. Gohlke, D. Weise, U. Johann, A. Peters, and C. Braxmaier, Class. Quantum Grav. **26**, 085008 (2009).
- [20] TLB-6800, *TLB-6800 Velocity Widely Tunable Lasers*, Datasheet DS-051202(07/14) (New Focus, 2014).
- [21] Iodine Frequency Stabilization, *Absolute Frequency, Ultra-Narrow Linewidth CW DPSS Laser System*, Datasheet MC-015-13-1M0113 (COHERENT, 2013).
- [22] O. Gerberding, C. Diekmann, J. Kullmann, M. Tröbs, I. Bykov, S. Barke, N. C. Brause, J. J. Esteban Delgado, T. S. Schwarze, J. Reiche, K. Danzmann, T. Rasmussen, T. V. Hansen, A. Enggaard, S. M. Pedersen, O. Jennrich, M. Suess, Z. Sodnik, and G. Heinzel, Review of Scientific Instruments **86**, 074501 (2015).
- [23] M. Lieser, Internal communication, 2016.
- [24] M. Dehne, *Construction and noise behaviour of ultra-stable optical systems for space intererometers*, Ph.D. thesis, Leibniz Universität Hannover (2012).
- [25] C. J. Killow, E. D. Fitzsimons, M. Perreux-Lloyd, D. I. Robertson, H. Ward, and J. Bogenstahl, Appl. Opt. **55**, 2724 (2016).